Development 135, 111-121 (2008) doi:10.1242/dev.009068

Oocyte regulation of metabolic cooperativity between mouse cumulus cells and oocytes: BMP15 and GDF9 control cholesterol biosynthesis in cumulus cells

You-Qiang Su[1], Koji Sugiura[1], Karen Wigglesworth[1], Marilyn J. O'Brien[1], Jason P. Affourtit[1], Stephanie A. Pangas[2], Martin M. Matzuk[2,3,4] and John J. Eppig[1,*]

Oocyte-derived bone morphogenetic protein 15 (BMP15) and growth differentiation factor 9 (GDF9) are key regulators of follicular development. Here we show that these factors control cumulus cell metabolism, particularly glycolysis and cholesterol biosynthesis before the preovulatory surge of luteinizing hormone. Transcripts encoding enzymes for cholesterol biosynthesis were downregulated in both *Bmp15*$^{-/-}$ and *Bmp15*$^{-/-}$ *Gdf9*$^{+/-}$ double mutant cumulus cells, and in wild-type cumulus cells after removal of oocytes from cumulus-cell-oocyte complexes. Similarly, cholesterol synthesized de novo was reduced in these cumulus cells. This indicates that oocytes regulate cumulus cell cholesterol biosynthesis by promoting the expression of relevant transcripts. Furthermore, in wild-type mice, *Mvk, Pmvk, Fdps, Sqle, Cyp51, Sc4mol* and *Ebp,* which encode enzymes required for cholesterol synthesis, were highly expressed in cumulus cells compared with oocytes; and oocytes, in the absence of the surrounding cumulus cells, synthesized barely detectable levels of cholesterol. Furthermore, coincident with reduced cholesterol synthesis in double mutant cumulus cells, lower levels were also detected in cumulus-cell-enclosed double mutant oocytes compared with wild-type oocytes. Levels of cholesterol synthesis in double mutant cumulus cells and oocytes were partially restored by co-culturing with wild-type oocytes. Together, these results indicate that mouse oocytes are deficient in synthesizing cholesterol and require cumulus cells to provide products of the cholesterol biosynthetic pathway. Therefore, oocyte-derived paracrine factors, particularly, BMP15 and GDF9, promote cholesterol biosynthesis in cumulus cells, probably as compensation for oocyte deficiencies in cholesterol production.

KEY WORDS: BMP15, GDF9, Mouse oocyte, Cumulus cells, Metabolism, Sterol biosynthesis, Gene expression

INTRODUCTION

Bi-directional communication between oocytes and companion somatic cells is essential for the development and function of ovarian follicles and promotes the production of mature oocytes competent to undergo fertilization, preimplantation development and development to term. Although granulosa cells provide essential nutrients and stimuli for oocyte growth and development, oocytes are not merely passive recipients of such support, but rather active regulators of follicular development. Oocytes affect the development and function of all stages of follicles beginning with the formation of primordial follicles (Soyal et al., 2000). Oocytes promote the primary to secondary follicle transition (Dong et al., 1996; Elvin et al., 1999b; Galloway et al., 2000; Juengel et al., 2002; Latham et al., 2004), granulosa cell proliferation and differentiation before the luteinizing hormone (LH) surge (Gilchrist et al., 2003; Gilchrist et al., 2000; Gilchrist et al., 2001; Otsuka et al., 2005; Otsuka et al., 2000; Vanderhyden et al., 1992; Vitt et al., 2000), the preantral to antral follicle transition (Diaz et al., 2007a; Diaz et al., 2007b; Orisaka et al., 2006) and cumulus expansion and ovulation after the LH surge (Buccione et al., 1990; Diaz et al., 2006; Dragovic et al., 2005; Dragovic et al., 2007; Joyce et al., 2001; Su et al., 2004; Vanderhyden et al., 1990).

[1]The Jackson Laboratory, 600 Main Street, Bar Harbor, ME 04609, USA. Departments of [2]Pathology, [3]Molecular and Cellular Biology, and [4]Molecular and Human Genetics, Baylor College of Medicine, Houston, TX 77030, USA.

*Author for correspondence (e-mail: john.eppig@jax.org)

Accepted 1 October 2007

Recently emerging evidence points to the existence of an oocyte-granulosa cell regulatory loop by which complementary signaling and metabolic pathways drive the development and function of both the oocytes and follicular somatic compartments. For example, *Slc38a3*, which encodes a sodium-coupled neutral amino acid transporter, and *Aldoa*, *Eno1*, *Ldha*, *Pfkp*, *Pkm2* and *Tpi1,* encoding enzymes in the glycolytic pathway, are highly expressed in cumulus cells compared with mural granulosa cells, and their expression in cumulus cells is promoted by oocyte-derived paracrine factors (Eppig et al., 2005; Sugiura et al., 2005). Moreover, the uptake of L-alanine and L-histidine, two preferred substrates of SLC38A3 (Gu et al., 2000), and the activity of glycolysis in cumulus cells, are promoted by factors secreted by fully grown oocytes at the germinal vesicle stage (Eppig et al., 2005; Sugiura et al., 2005). Since oocytes themselves are unable to take up L-alanine and poorly metabolize glucose for energy production, they obtain these amino acids and products of glycolysis, which are essential for their development and function, from cumulus cells (Biggers et al., 1967; Colonna and Mangia, 1983; Donahue and Stern, 1968; Eppig et al., 2005; Haghighat and Van Winkle, 1990; Leese and Barton, 1984; Leese and Barton, 1985). Thus, oocytes benefit their own development by enhancing metabolic cooperativity between granulosa cells and oocytes (for a review, see Sugiura and Eppig, 2005).

Growth differentiation factor 9 (GDF9) and bone morphogenetic protein 15 (BMP15) are two well-characterized oocyte-derived growth factors that play crucial roles in follicle growth and ovulation in all mammalian species studied, including rodents (Dong et al., 1996; Elvin et al., 1999b; Yan et al., 2001), domestic ruminants (Bodin et al., 2007; Galloway et al., 2000; Juengel et al., 2002) and humans (Chand et al., 2006; Di Pasquale et al., 2006; Dixit et al., 2006; Palmer

et al., 2006). GDF9 and/or BMP15 are probably major players of the 'oocyte-granulosa cell regulatory loop', and participate in many of the aforementioned functions of oocytes (for reviews, see Eppig, 2001; Erickson and Shimasaki, 2001; Matzuk et al., 2002; McNatty et al., 2004). Genetic targeting or spontaneous mutations of either *Gdf9* or *Bmp15* in mammals affect fertility in females (for reviews, see Juengel and McNatty, 2005; Pangas and Matzuk, 2004). Particularly in mice, deletion of *Gdf9* by homologous recombination (*Gdf9*^{tm1Zuk}/*Gdf9*^{tm1Zuk}, hereafter *Gdf9*$^{-/-}$) causes arrest of folliculogenesis at the primary stage and female infertility since the cuboidal granulosa cells fail to proliferate (Dong et al., 1996; Elvin et al., 1999b). Deletion of *Bmp15* (*Bmp15*^{tm1Zuk}/*Bmp15*^{tm1Zuk}, hereafter *Bmp15*$^{-/-}$) results in reduced female fertility with the primary defects in ovulation and fertilization (Yan et al., 2001). A more dramatic reduction of fertility was observed in double mutant *Bmp15*$^{-/-}$*Gdf9*$^{+/-}$ (hereafter DM) than in *Bmp15*$^{-/-}$ females. The cumuli oophori ovulated in DM females are fragile and unstable (Yan et al., 2001) indicating that GDF9 and BMP15 are essential for the normal development of cumulus-oocyte complexes (COCs). Although in-vitro studies using recombinant GDF9 and BMP15 demonstrate that both growth factors, either alone or in combination, play significant role(s) at all stages of follicular development (Elvin et al., 1999a; Elvin et al., 2000; Hayashi et al., 1999; Hussein et al., 2005; McNatty et al., 2005a; McNatty et al., 2005b; Otsuka et al., 2001a; Otsuka and Shimasaki, 2002; Otsuka et al., 2001b; Otsuka et al., 2000; Vitt et al., 2000), controversy persists owing to differences in recombinant protein preparations (for a review, see Pangas and Matzuk, 2005). It has been suggested that the role of BMP15 in mouse follicular development is restricted to the period after the LH surge (Gueripel et al., 2006; Li et al., 2006; Yoshino et al., 2006). These studies are contradicted by evidence that cumuli oophori of DM mice are abnormal even before the LH surge because they are unable to undergo normal expansion in vitro even when co-cultured with normal wild-type oocytes (Su et al., 2004). However, the extent of the role of BMP15 in the differentiation and function of cumulus cells before the LH surge is unknown.

The first objective of the present study was to determine the effects of BMP15 and GDF9 on cumulus cells before the LH surge by analyzing the transcriptomes of cumulus cells from wild-type (WT), *Bmp15*$^{-/-}$ and DM mice using microarrays and bioinformatics methods. We report that cumulus cell metabolic pathways, particularly glycolysis and cholesterol biosynthesis, are highly affected by *Bmp15* and *Gdf9* mutation. To follow up on these findings, we conducted a detailed analysis of cholesterol biosynthesis in oocytes and cumulus cells and the ability of oocytes to promote the cholesterol biosynthetic pathway in cumulus cells.

MATERIALS AND METHODS

Mice

Adult (4- to 5-month-old) female *Bmp15*$^{-/-}$ and DM mice on the B6/129 genetic background and similarly aged WT B6129F1 mice produced in the research colonies of the authors were used for the microarray and the subsequent real-time PCR validation experiments. Other experiments were conducted with normal 22- to 24-day-old female B6SJLF1 mice. All animal protocols were approved by the Administrative Panel on Laboratory Animal Care at The Jackson Laboratory, and all experiments were conducted in accordance with the NIH Guide for the Care and Use of Laboratory Animals.

Cumulus cell isolation

Female WT, *Bmp15*$^{-/-}$ and DM mice were primed with 7.5 IU equine chorionic gonadotropin (eCG, EMD Biosciences, Calbiochem, La Jolla, CA) for 48 hours to stimulate follicular development. Cumulus-cell-oocyte complexes (COCs) were released by puncturing large antral follicles with a pair of 26-gauge needles. Released COCs were collected and washed three times by passing through three dishes of medium. Cumulus cells were then stripped off oocytes by passing COCs several times through a glass pipette with an inner diameter slightly narrower than the oocyte. After removing all of the denuded oocytes from the dish, cumulus cells were transferred into a 1.5 ml centrifuge tube, and collected by gentle centrifugation. The resulting pellets were resuspended in 350 μl RLT buffer (Qiagen, Valencia, CA) after removing the supernatant, and were snap frozen in liquid nitrogen and temporarily stored at –80°C until RNA isolation. Three sets of WT, *Bmp15*$^{-/-}$ and DM cumulus cell samples were collected and employed in this microarray study. For each sample, about 75-100 COCs, obtained from 3-4 mice, were used for cumulus cell collection. Four additional sets of cumulus cell samples were collected and used for subsequent real-time RT-PCR analysis. Medium used for cumulus cell isolation was MEM-α (Invitrogen Corporation, Grand Island, NY) supplemented with 3 mg/ml crystallized lyophilized bovine serum albumin (Sigma, St Louis, MO), 75 mg/l penicillin G (Sigma) and 50 mg/l streptomycin sulfate (Sigma). Milrinone (Sigma), a selective inhibitor of oocyte-specific phosphodiesterase (PDE3), was added into the medium at a concentration of 5 μM to prevent the fully grown GV-stage oocytes from undergoing maturation during the process of COC and cumulus cell isolation and culture.

RNA sample preparation and array processing

Total RNA was extracted from cumulus cells using the RNeasy Micro Kit (Qiagen) according to the manufacturer's instructions. The RNA quality and yield of each sample were determined using the Bioanalyzer 2100 and RNA 6000 Pico LabChip assay (Agilent Technologies, Palo Alto, CA) in combination with Quant-iT RiboGreen Reagent according to supplied protocols (Invitrogen). Total RNA (10 ng) isolated from each sample was used in the two-round cDNA synthesis and subsequent in vitro-transcription according to the Two-Cycle Eukaryotic Target Labeling Assay [Affymetrix Expression Analysis Technical Manual: Section 2: Eukaryotic Sample and Array Processing (http://www.affymetrix.com/support/technical/manual/expression_manual.affx)]. Equal amounts (15 μg) of fragmented and biotin-labeled cRNA from each sample were then hybridized to Affymetrix GeneChip Mouse Genome 430 2.0 Arrays for 16 hours at 45°C. Post-hybridization staining and washing were performed according to manufacturer's protocols using the Fluidics Station 450 instrument (Affymetrix).

Image acquisition, quantification and microarray data analysis

After post-hybridization staining and washing, the arrays were scanned with a GeneChip 3000 laser confocal slide scanner (Affymetrix) and the images were quantified using Gene Chip Operating Software version 1.2 (GCOS, Affymetrix). Probe level data were imported into the R software environment and expression values were summarized using the RMA (Robust MultiChip Average) function (Irizarry et al., 2003) in the R/affy package (Gautier et al., 2004). Using the R/maanova package (Wu, 2003), an analysis of variance (ANOVA) model was applied to the data, and Fs test statistics were constructed along with their permutation *P*-values (Cui and Churchill, 2003; Cui et al., 2005). False discovery rate (FDR) (Storey and Tibshirani, 2003) was then assessed using the R/qvalue package to estimate q-values from calculated Fs test statistics. Three pairwise comparison analyses: DM vs WT, *Bmp15*$^{-/-}$ vs WT, and DM vs *Bmp15*$^{-/-}$, were generated, and the significantly changed transcripts were identified using the criteria of Fs $P<0.01$. Results were annotated using information provided by Affymetrix (12/20/2005 release). Full data sets are available at http://www.ncbi.nlm.nih.gov/geo/ (Acc. no. GSE7225).

Pathway analysis

Gene identifiers and their corresponding Fs p-values, and fold changes were uploaded into IPA 3.1 (Ingenuity Pathway Analysis, Ingenuity System, http://www.ingenuity.com) and GenMAPP 2.0 (Gene Map Annotator and Pathway Profiler, http://www.genmapp.org)/MAPPFinder 2.0 to identify the pathways and functions associated with significantly changed transcripts.

Real-time RT-PCR analysis

Real-time RT-PCR analyses were carried out using total RNA isolated from target cells (cumulus cells or oocytes). RNA isolation was accomplished using the RNeasy Micro Kit (Qiagen). In vitro transcription was carried out using

Table 1. Primer sets used for real-time RT-PCR

Gene symbol	RefSeq Acc. no.	Forward primer sequence (5′-3′)	Reverse primer sequence (5′-3′)	Amplicon position	Amplicon size (bp)
Adhfe1	NM_175236	TTTGCCATGCTCTGGAGTCAT	ATGTCGCTGATTGGGTTGCT	739-850	112
Ak3l1	NM_009647	GACAAACCAGAGACAGTGATCAAGAG	GAGAATGTTTCCAACACCCCTTT	563-663	101
Aldoc	NM_009657	GAACAAAAGGAGATGTGGGAACTG	AGCAGGAGAAGCAGCCTTTGG	4-107	104
Aox4	NM_009676	GCGCCCTCCAGAAACATCT	AAATTAGGACGGCTTGCAGTGT	1112-1202	91
Bmp2	NM_007553	GACGTCCTCAGCGAATTTGAGT	GCCTGCGGTACAGATCTAGCATA	299-413	115
Ceacam10	NM_007675	GTTCACGCTAAAAAGCAGTAGGAAT	VAGAGTTTCGGTTCCAGTTAGAAAGA	871-961	91
Cyp27a1	NM_024264	GGAGGGCAAGTACCCAATAAGAG	TTGTGCGATGAAGATCCCATAG	424-514	91
Cyp51	NM_020010	GGCAAGACCTTCACTTACCTTCTG	GACCGTAGACTTCTTCTGCATTCAG	694-787	94
Dapk1	NM_029653	GCAGGAAAACGTGGACGACTAC	AACTTGGCCGCATACTGAAGAC	124-237	114
Dhcr7	NM_007856	GTCCAAGAAGGTGCCATTACTCC	GCGTTCACAAACCAGAGGATGT	880-980	101
Ebp	NM_007898	CAACAGCCCTTCCGCTTTG	CCCATGCTGGAGTCCTTCGT	1196-1300	105
Egr3	NM_018781	TCAGATGGCTACAGAGAATGTGATG	CCAAGTAGGTCACGGTCTTGTTG	141-259	119
Fdft1	NM_010191	GGACATACGGCACGCCATAT	GGGATCTTCTTCTCCACACTGATG	201-296	96
Fdps	NM_134469	TGTGTAGAACTGCTCCAGGCTTT	AAGCCTATGCCTGGCTTCTGA	377-483	107
Gpr155	NM_001080707	CAGACAGAGAATCCCCCGTTT	GTCTTGGCACCACACCCTCCTT	631-748	118
Hmgcr	NM_008255	TGAACATGATCTCTAAGGGTACGGA	TGTCGGTGCAATAGTTCCCACT	2028-2129	102
Idi1	NM_145360	AAGCCGAGTTGGGAATACCCT	GTTCACCCCAGATACCATCAGATT	381-482	102
Igfbp1	NM_008341	GCCAAACTGCAACAAGAATGG	AGACCCAGGGATTTTCTTTCCA	851-968	118
Lss	NM_146006	GTGATGCAGGCACTGAAGCA	GCAGAAGTCCAGGCCTTGATT	1646-1738	93
Mvd	NM_138656	TCTACCCCTCAGCCTCAGCTATAA	AGGGTATAGGCTAGGCAGGCATA	330-440	111
Mvk	NM_023556	ATCCATGGGAACCCTTCTGG	GACGGGAGGCTCTTCAAGGA	658-758	101
Nsdhl	NM_010941	ATGCAGCTAGAAAGGGCAAAATG	GGCTAAGATGTGTCCATGAACCAC	832-932	101
Pfkl	NM_008826	CCCTTTCGACCGGAACTATGG	CCGCCCTTTACGGTAGACATC	2072-2162	91
Pmvk	NM_026784	AGCAGAGTCGACAGCAACGG	TCTCAATGACCCAGTCAAAGTTCC	459-563	105
Rpl19	NM_009078	CCGCTGCGGGAAAAAGAAG	CAGCCCATCCTTGATCAGCTT	45-147	103
Sc4mol	NM_025436	CACAGACTCCTTCACCACAAGAGAA	TTTCCAAGGGATGTGCGTATTC	571-676	106
Sc5d	NM_172769	AGCATCCCCACCGTCTCACT	CGACGCTAACCATGAGATGAATC	379-487	109
Sqle	NM_009270	AGCTATGGCAGAGCCCAATGTA	AGGTGTTGTGCTTCAGTTACTAGAGGAA	1455-1546	92
Tm7sf2	NM_028454	AGCTTGGGTACCATTCACCTACAG	GGCCCCTCGGAACATGTAGT	914-1043	130

QuantiTect Reverse Transcription Kit (Qiagen) at 42°C for 15 minutes. Real-time PCR was then conducted to quantify the steady-state mRNA levels of the tested genes using QuantiTect SYBR Green PCR Kits (Qiagen) on the ABI 7500 Real-time PCR System (Applied Biosystems, Foster City, CA). The threshold cycle (Ct) was used for determining the relative expression level of each gene by normalizing to the Ct of *Rpl19* mRNA. The method of 2^{-ddCt} was used to calculate relative fold change of each gene as described previously (Su et al., 2007). To ensure only target gene sequence-specific, non-genomic products were amplified by real-time PCR, careful design and validation of each primer pair, as well as cautious manipulation of RNA were undertaken as described exactly in previous studies (Su et al., 2007). Primers used for real-time PCR are shown in Table 1.

Oocytectomy (OOX) and co-culture of OOX cumulus cells with oocytes

COCs were isolated from 22-day-old eCG-primed B6SJLF1 mice. Microsurgical oocytectomy (OOX) was carried out as described previously (Buccione et al., 1990). Fully-grown oocytes were isolated from the same age eCG-primed B6SJLF1 mice as described previously (Su et al., 2007). COCs, OOX cumulus cells (without oocytes) and OOX cumulus cells + oocytes (two fully grown oocytes/μl medium) were cultured in a drop of medium covered with mineral oil at a density of one COC or OOX cumulus cell/μl medium in a four-well plate (Nuclon, Denmark). Medium used for culture was the same as that used for mutant cumulus cell isolation. Cells were cultured at 37°C in a modular incubation chamber (Billups Rothenberg, Del Mar, CA) infused with 5% O_2, 5% CO_2 and 90% N_2 for 20 hours, and then were collected in RTL buffer for RNA isolation.

In situ hybridization

In situ hybridization was performed using ovarian sections derived from eCG-primed (44-46 hours) B6SJLF1 mice as described previously (Eppig et al., 2002). ^{33}P-labeled cRNA probes were prepared using target gene-specific PCR products amplified from cDNA of B6SJLF1 ovaries. The length and region of probes were: *Mvk*, 859 bp, NM_023556, 604-1462; *Fdps*, 1018 bp, NM_134469, 16-1033; *Sqle*, 809 bp, NM_009270, 1364-2172; *Cyp51*, 1205 bp, NM_020010, 730-1934; *Sc4mol*, 806 bp, NM_025436, 428-1233.

Analysis of de-novo cholesterol biosynthesis

Levels of cholesterol in cumulus cells and/or oocytes were compared by assessing the incorporation of [1-^{14}C]acetate into cholesterol using a protocol adapted from previous reports (Friberg et al., 2007; Rung et al., 2006; Rung et al., 2005). Briefly, for comparing cholesterol synthesis in WT, *Bmp15*$^{-/-}$, and DM COCs, 150 COCs of each genotype were cultured in medium supplemented with 10 μCi [1-^{14}C]acetic acid, sodium salt (Amersham Biosciences, Buckinghamshire, UK) for 5 hours. For testing the effects of OOX on cholesterol synthesis in WT cumulus cells, 150 COCs, OOX cumulus cells or OOX cumulus cells + oocytes were initially cultured in a drop of radioisotope-free medium covered by mineral oil at a density of 1 COC or OOX cumulus cell/μl medium in a four-well plate for 15 hours, and then transferred to fresh medium (375 μl/well) where cumulus cells of the intact COC group were stripped off and oocytes discarded. Finally, 10 μCi (50 μl) [^{14}C]acetate was added and cells were cultured for additional 5 hours. At the end of culture, cells and media were collected, and cholesterol in the cells and media was extracted and subjected to thin layer chromatography (TLC). For comparing the levels of cholesterol synthesized in WT cumulus-enclosed oocytes and denuded oocytes, 400 cumulus-cell-enclosed and denuded oocytes were incubated with 10 μCi [^{14}C]acetate in 425 μl medium for 5 hours. They were washed four times in 2.5 ml fresh medium. After washing, the cumulus-cell-enclosed oocytes were denuded, and resultant oocytes were collected for cholesterol extraction. Equal numbers of oocytes were also collected from the denuded oocyte group incubated without cumulus cells, and subjected to cholesterol extraction and TLC separation.

To compare levels of cholesterol synthesized in WT and DM cumulus-enclosed oocytes, and to test effects of co-culturing with fully-grown WT oocytes on cholesterol synthesis in DM cumulus cells and oocytes, 100 WT and DM COCs or 100 DM COCs + WT oocytes (four oocytes/μl medium) were initially cultured in a drop of medium covered by mineral oil at a density of one COC/μl of medium in a four-well plate for 15 hours. Then 2.5 μCi [^{14}C]acetate was added and cultured for an additional 5 hours. At the end of culture, complexes were washed four times in 2.5 ml fresh medium, and cumulus-cell-enclosed oocytes were denuded, and resultant oocytes and cumulus cells were collected. For each TLC run, oocytes collected from four

independent experiments, each containing 100 oocytes, were pooled to produce a total of 400 denuded oocytes, and cholesterol was extracted. This experiment was then replicated four times.

Unlabeled cholesterol (10 μg) was added to each sample at the beginning of cholesterol extraction to serve as a carrier and external control. The TLC plates were silica gel 60, 20×20 cm (Merck, Darmstadt, Germany). Compounds in extracted samples were separated on TLC plates using a mobile phase solvent mixed of petroleum ether:diethyl ether:acetic acid (60:40:1, v/v). Bands separated on plates were visualized using iodine (Sigma, Grand Island, NY) staining. Unlabeled cholesterol (10 μg) was loaded directly on the plate in a separate lane to identify the location of radioisotope-labeled cholesterol bands. Dried plates were placed onto Fuji Phosphor Imaging Plates (Fuji Medical Systems USA, Stamford, CT), and exposed for at least 2 days, scanned using a Fuji Phosphor Imager (Fuji Medical Systems USA), and the intensity of each corresponding cholesterol band quantified using Fuji Phosphor Imaging system software (Fuji Medical Systems USA).

Statistical analysis

All experiments were repeated at least three times independently, and data are presented as mean ± s.e.m. Student's *t*-test was conducted to evaluate differences when there were only two groups. For experiments with more than two groups of treatments, one-way ANOVA followed by Tukey's HSD test was used to evaluate differences between groups using JMP software (SAS Institute, Cary, NC). $P<0.05$ was considered significantly different.

RESULTS

Dramatic changes in transcript profiles of cumulus cells from *Bmp15*$^{-/-}$ and DM mice

Three pairwise comparisons, DM vs WT, *Bmp15*$^{-/-}$ vs WT and DM vs *Bmp15*$^{-/-}$, identified the most highly affected transcripts in mutant cumulus cells. As shown in Fig. 1, compared with WT, there were 7640 and 5332 unique transcripts whose levels of expression were significantly changed in DM and *Bmp15*$^{-/-}$ cumulus cells, respectively. Interestingly, when compared with WT, there were 4147 (2958 + 1189, 54.3%) and 1839 (1522 + 317, 34.5%) transcripts whose expression was changed only in DM or *Bmp15*$^{-/-}$ cumulus cells, respectively (Fig. 1). Since these transcripts were not commonly changed in the two groups, they are regulated in cumulus cell either by the full complement of GDF9 and BMP15, or only by BMP15. There were 744 transcripts commonly altered in all three pairwise comparisons (Fig. 1) and these were considered the transcripts most highly affected by mutations of *Bmp15* and *Gdf9* and were used for bioinformatic pathways and functions analyses.

Validation of the microarray data by real-time RT-PCR

Validation of data was carried out on two groups of selected transcripts using quantitative real-time RT-PCR (Fig. 2). The first group of transcripts was representative of those whose steady-state levels appeared highly changed in DM (Fig. 2A,B) and *Bmp15*$^{-/-}$ (Fig. 2F,G) cumulus cells by microarray analysis. The second group was representative of those in DM (Fig. 2C,D,E) and *Bmp15*$^{-/-}$ (Fig. 2H,I,J) cumulus cells involved in specific metabolic pathways described in the following section (see Fig. 3). In all cases, quantitative differences between groups were similar in both microarray and RT-PCR data, thus validating use of microarray data for further bioinformatic analyses and testing of physiological mechanisms.

Pathways and functions associated with the transcripts most highly affected by mutations of *Bmp15* and *Gdf9*

To identify biological themes underlying effects of the mutations on transcript levels in cumulus cells, IPA and GenMAPP/MAPPFinder bioinformatic packages were used to carry out pathway and function

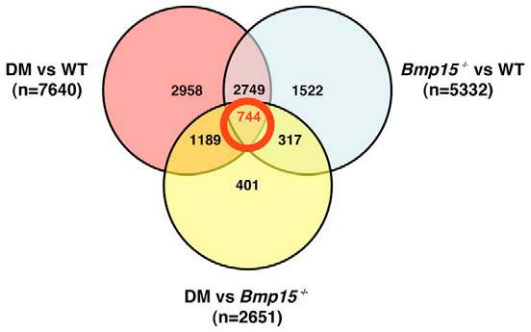

Fig. 1. Venn diagram illustrating the number of unique transcripts whose steady-state level of expression is changed in mutant cumulus cells. Numbers indicate the number of transcripts (Unigene IDs) whose levels are changed significantly in pairwise comparisons. Overlapping areas of two or three circles represent the number of transcripts whose levels are commonly changed in the corresponding two- or three-comparison tests.

analyses on the 744 transcripts whose levels of expression were commonly affected in the mutant groups as shown in Fig. 1. As shown in Fig. 3A, seven canonical pathways (of 113 in the IPA pathway library) were significantly affected. Surprisingly, all pathways identified were metabolic and the majority of changed transcripts involved in these pathways were downregulated in mutant cumulus cells. When IPA analysis was conducted using only downregulated transcripts, the same pathways were found to be significantly affected as when all the changed transcripts were used. No pathways were significantly affected when only upregulated transcripts were used in the IPA analysis. Of the seven identified pathways, glycolysis/gluconeogenesis and sterol biosynthesis were the two pathways most affected. As shown in Fig. 3C (and see Fig. S1 in the supplementary material), most of the transcripts encoding enzymes for sterol biosynthesis and glycolysis/gluconeogenesis, respectively, were downregulated in *Bmp15*$^{-/-}$ and DM cumulus cells.

IPA also identified 25 categories of molecular and cellular functions that were associated with the 744 transcripts. The 10 most affected are shown in Fig. 3B. Lipid metabolism and small molecule biochemistry were the most highly affected functions and cholesterol biosynthesis (sterol biosynthesis) was the major subcategory of these two functions (see Tables S1 and S2 in the supplementary material). Canonical pathways and molecular and cellular functions identified by IPA were essentially the same as those identified by GenMAPP/MAPPFinder analyses as downregulated in the mutant cumulus cells (see Tables S3 and S4 in the supplementary material).

Effect of WT oocytes on expression of selected transcripts in WT cumulus cells

Altered expression of transcripts in mutant cumulus cells may be the result of chronic deficiencies in BMP15 and/or GDF9 throughout follicular development and may not reflect the acute regulatory response of cumulus cells to oocyte-derived factors. To address this possibility, we tested the effects of WT oocytes on expression of transcripts by WT cumulus cells cultured for only 20 hours. Transcripts chosen for analysis were those whose levels of expression were affected in *Bmp15*$^{-/-}$ and DM cumulus cells and validated in experiments shown in Fig. 2, with emphasis given to transcripts encoding enzymes of the cholesterol biosynthesis pathway. As shown in Fig. 4, for all selected transcripts, OOX resulted in a pattern of

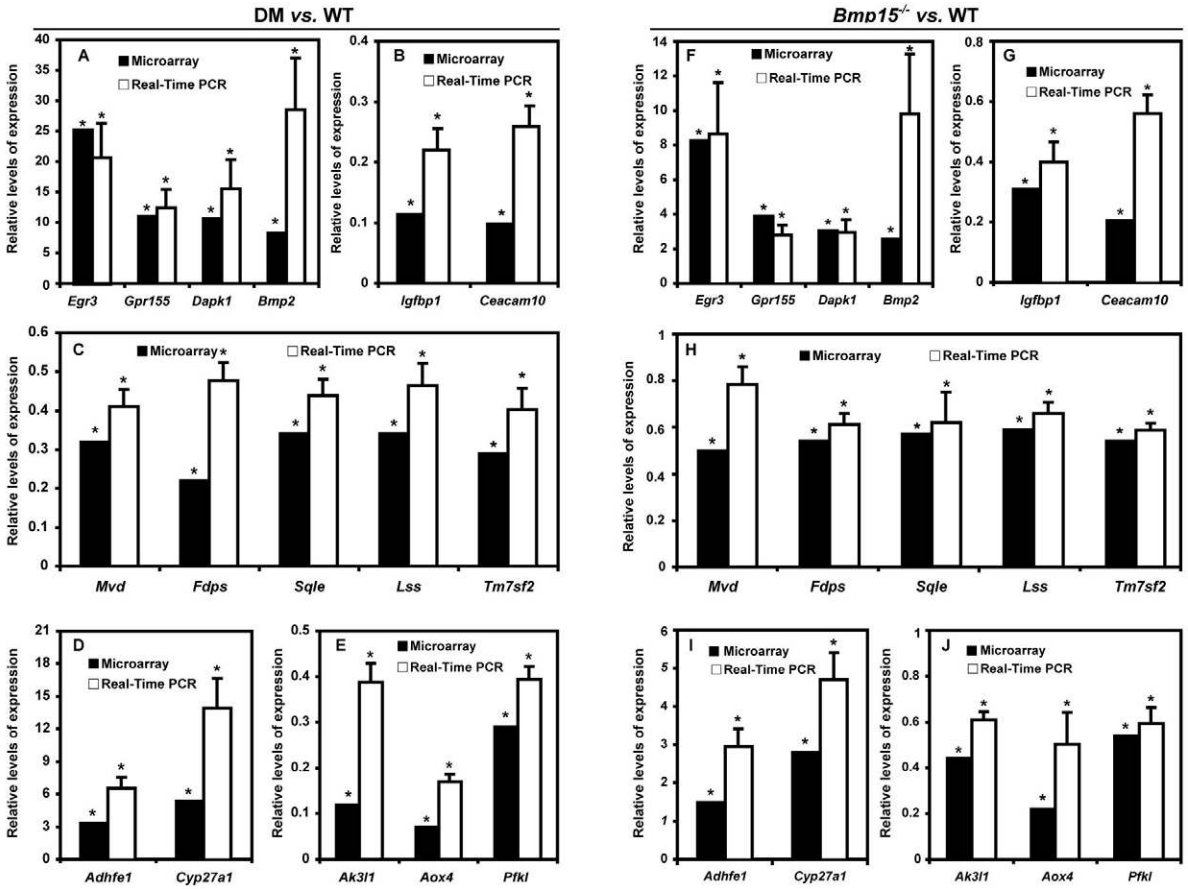

Fig. 2. Real-time RT-PCR analysis of transcripts selected from microarray expression profiles. (**A-J**) Five categories of transcripts were selected for real-time RT-PCR analysis: transcripts that were most dramatically up- (A,F), or down- (B,G) regulated in mutant cumulus cells; transcripts that were specifically involved in certain metabolic pathways, e.g. sterol biosynthesis (C,H), bile acid biosynthesis (D,I), and glycolysis, purine metabolism, pyrimidine metabolism, pentose phosphate, and fructose and mannose metabolism (E,J). Black bars indicate expression levels detected by microarray, white bars indicate levels detected by real-time RT-PCR. Four sets of cumulus cell samples from each genotype were used for real-time PCR analysis and data are presented as mean ± s.e.m. of fold changes. *P<0.05; DM vs WT, or *Bmp15*$^{-/-}$ vs WT.

mRNA expression in WT cumulus cells that was similar to that in mutant cumulus cells. Co-culture of OOX cumulus cells with WT oocytes prevented these changes. Specifically, OOX caused a dramatic increase in the expression of the transcripts whose levels were upregulated in *Bmp15*$^{-/-}$ and DM cumulus cells, and this change was prevented by co-culture of OOX cumulus cells with WT oocytes (Fig. 4A). OOX also dramatically reduced expression of transcripts whose levels of expression were downregulated in *Bmp15*$^{-/-}$ and DM cumulus cells, and this reduction did not occur when oocytes were present (Fig. 4B). Most interestingly, of the 16 transcripts selected from the 17 transcripts encoding enzymes for cholesterol biosynthesis, 15 were found to be expressed at significantly lower levels in OOX cumulus cells than in cumulus cells of intact COCs (Fig. 4C). Co-culture of OOX cumulus cells with WT oocytes sustained elevated steady-state expression of these transcripts. Similar changes were observed for transcripts encoding enzymes involved in other metabolic pathways, i.e. glycolysis, purine metabolism, pyrimidine metabolism, pentose phosphate, fructose and mannose metabolism and inositol metabolism (Fig. 4E). In contrast to the downregulation of transcripts encoding enzymes required for cholesterol biosynthesis in OOX cumulus cells, a dramatic upregulation of *Cyp27a1* mRNA encoding cholesterol 27 hydroxylase, which functions in cholesterol metabolism, was observed in OOX cumulus cells, and this upregulation was prevented by co-culture with oocytes (Fig. 4D).

Reduction of de-novo cholesterol synthesis in mutant COCs and WT OOX cumulus cells

We next determined whether the reduced expression of transcripts encoding enzymes in the cholesterol biosynthesis pathway reflects changes in cholesterol synthesis in cumulus cells. As shown in Fig. 5A,B, compared with WT COCs, levels of de-novo-synthesized cholesterol in *Bmp15*$^{-/-}$ and DM COCs were dramatically reduced, to about 55% and 25% of WT level, respectively. OOX resulted in more than a 90% reduction of de-novo synthesized cholesterol in WT OOX cumulus cells (Fig. 5C,D). Synthesis of cholesterol in OOX cumulus cells was elevated when they were co-cultured with WT oocytes. However, this increase was only to 50% of the control level (Fig. 5C,D).

Differences between cumulus cells and oocytes in expression of transcripts encoding enzymes required for cholesterol biosynthesis

Steady-state levels of transcripts encoding enzymes in the cholesterol biosynthesis pathway were compared in cumulus cells and oocytes obtained from WT mice. As shown in Fig. 6A, transcripts, *Mvk*, *Pmvk*, *Fdps*, *Sqle*, *Cyp51*, *Sc4mol* and *Ebp*, were expressed at much higher levels in cumulus cells than in oocytes, relative to levels of *Rpl19* mRNA in the respective cell types. Because possible differences in levels of *Rpl19* mRNA in oocytes

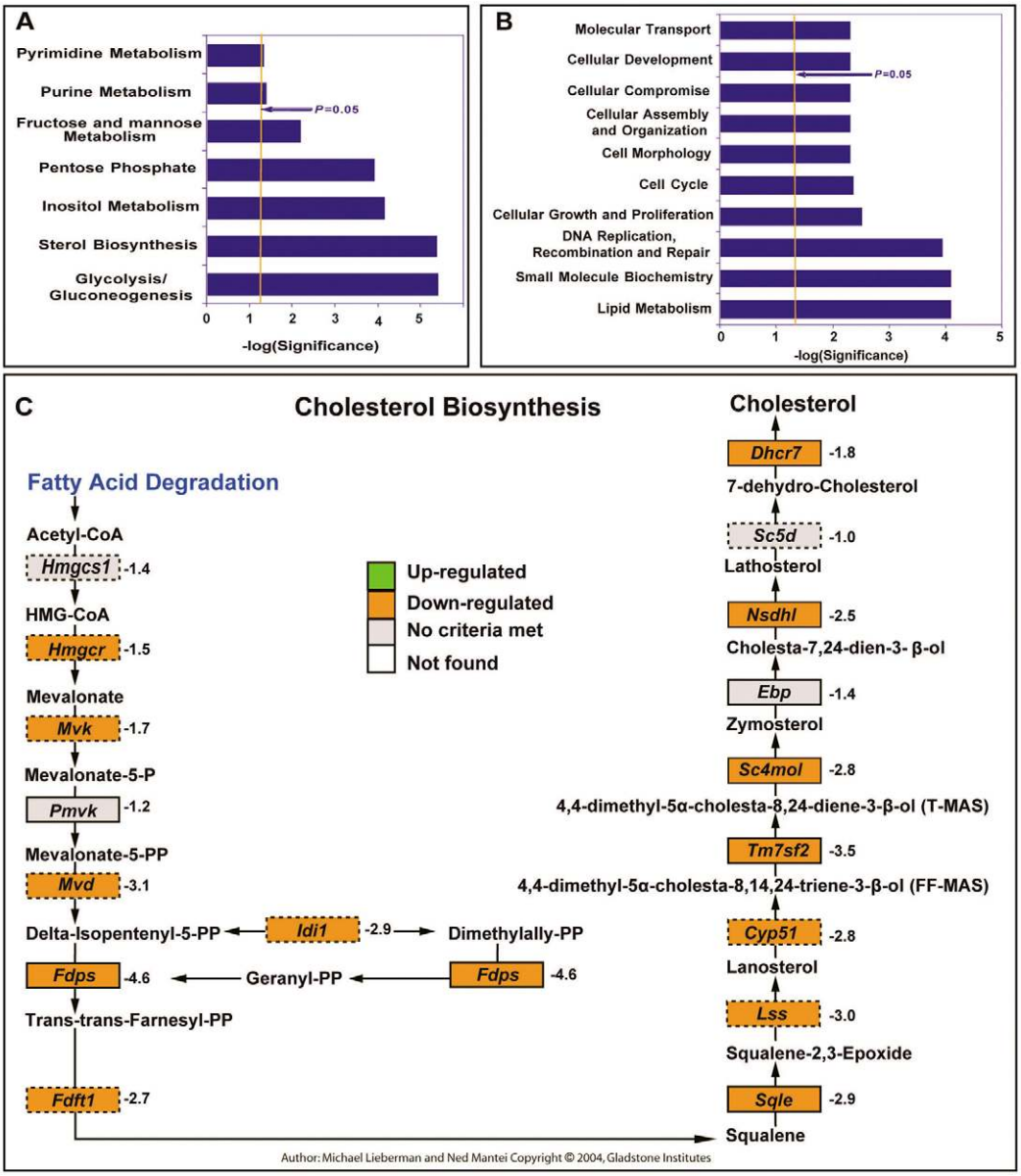

Fig. 3. The most highly affected pathways and functions in mutant cumulus cells. The 744 transcripts that were commonly changed in all three pairwise comparisons of cumulus transcriptomes in WT, *Bmp15*$^{-/-}$, and DM mice were uploaded into the IPA platform, and canonical pathways and molecular functions analyses were carried out using Ingenuity Pathways Knowledge Base as reference dataset. (**A**) All canonical pathways identified that were significantly affected. (**B**) The 10 most affected molecular functions. The orange vertical line crossing all the bars in A and B indicates the threshold of significance (P=0.05), and bars above this line have a P-value of less than 0.05. (**C**) GenMAPP display of transcripts encoding enzymes required for cholesterol biosynthesis pathway. The list of all the genes on the array was uploaded into GenMAPP, and significantly downregulated transcripts were defined by the criteria of FC (fold change) <–1 and Fs P<0.01 in all three pairwise comparison analyses, and are shown in orange boxes. Upregulated transcripts are defined by the criteria of FC>1 and Fs P<0.01 in all three pairwise comparison analyses. No transcripts are identified to be upregulated by these criteria. Dotted boxes indicate that the transcripts in these boxes are represented by >1 probe set. The FC of each transcript is listed on the right side of the corresponding box. Only the $FC_{DM\ vs\ WT}$ of each transcript is shown here owing to space limitation. Minor modification of the original MAPP in GenMAPP was made here in order to cover most of the key enzymatic steps in this pathway, such as steps for producing FF-MAS and T-MAS. Panel C, by Michael Lieberman and Ned Mantei (2004), is reproduced from GenMAPP.

and cumulus cells would bias this comparison, we compared expression by unbiased in situ hybridization. Robust levels of *Mvk*, *Fdps*, *Sqle*, *Cyp51*, and *Sc4mol* transcripts (Fig. 6B), and *Pmvk* and *Ebp* transcripts (not shown), were detected in cumulus cells, as well as the periantral granulosa cells, but not in oocytes (Fig. 6B). The results described above suggest that oocytes are deficient in sterol biosynthesis and require products of this pathway to be supplied by cumulus cells. To test this possibility, levels of cholesterol synthesized in cumulus-cell-enclosed oocytes and denuded oocytes were compared. After stripping cumulus cells from cumulus-cell-enclosed oocytes, >fivefold more radiolabeled cholesterol was found in cumulus-cell-enclosed than denuded oocytes (Fig. 7A). Differences between labeled cholesterol in denuded oocytes and cumulus-cell-enclosed oocytes could result from differences in

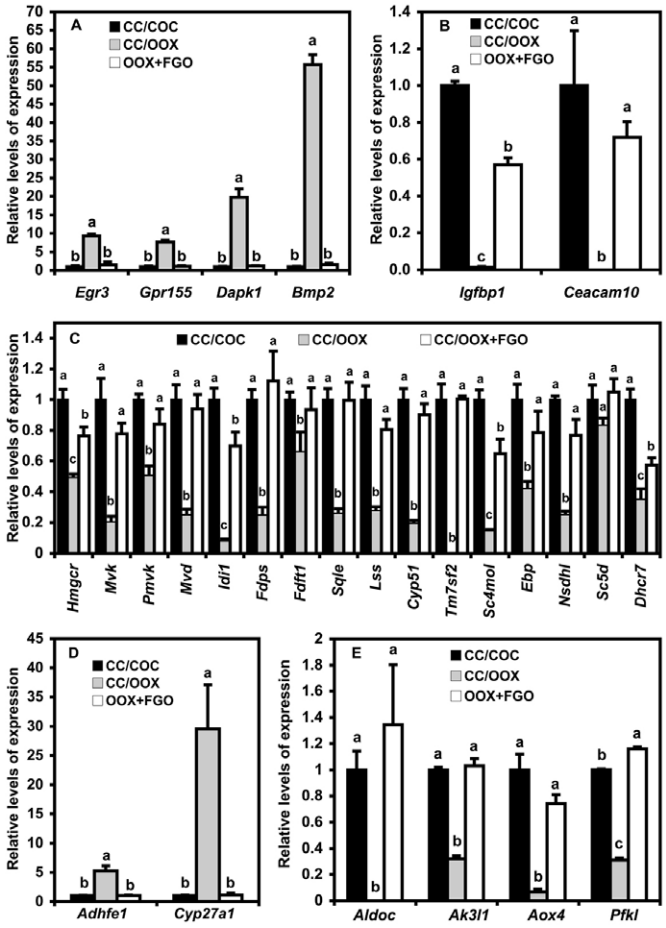

Fig. 4. Effect of WT oocytes on expression of selected transcripts in WT OOX cumulus cells. WT COCs, OOX cumulus cells, and OOX cumulus cells + oocytes [two fully grown oocytes (FGO)/μl] were cultured for 20 hours, and expression of selected transcripts was detected by real-time RT-PCR using *Rpl19* mRNA as internal control. (**A**) Transcripts upregulated in cumulus cells of both mutants. (**B**) Transcripts downregulated in cumulus cells of both mutants. (**C**) Transcripts encoding enzymes for cholesterol biosynthesis. (**D**) Transcripts involved in bile acid biosynthesis pathway. (**E**) Transcripts involved in other metabolic pathways: glycolysis, purine metabolism, pyrimidine metabolism, pentose phosphate, fructose and mannose metabolism, and inositol metabolism. Experiments were repeated three times. Data are presented as mean of the relative fold change in mRNA expression compared with COC group (control) ± s.e.m. Bars indicated with different letters are significantly different, $P<0.05$.

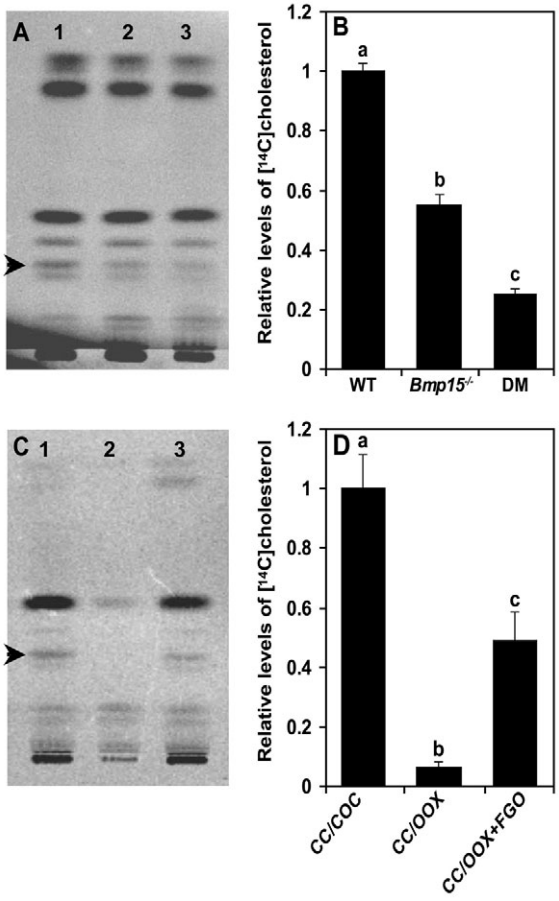

Fig. 5. Reduction of cholesterol synthesis in mutant COCs and WT OOX cumulus cells. Cholesterol synthesis was measured as incorporation of [^{14}C]acetate into cholesterol during culture. (**A**) A representative TLC image comparing radiolabeled cholesterol (indicated by arrow) in WT (lane1), *Bmp15*$^{-/-}$ (lane 2) and DM (lane 3) COCs. (**B**) Quantitative comparison of [^{14}C]cholesterol levels in WT and mutant COCs. (**C**) A representative TLC image showing relative [^{14}C]cholesterol (indicated by arrow) levels in WT cumulus cells of COCs (lane1), OOX cumulus cells (lane 2) and OOX cumulus cells + oocytes (lane 3). (**D**) Quantitative comparison of [^{14}C]cholesterol levels in WT cumulus cells of COCs, OOX cumulus cells and OOX cumulus cells + oocytes. All experiments were repeated at least three times independently. Data are presented as mean of relative fold change compared with control (WT in panels B, CC/COC in panels D) ± s.e.m. Bars indicated with different letters are significantly different, $P<0.05$.

availability of labeled acetate. Note, however, that the unidentified radiolabeled bands near the origin are about the same intensity in both groups (Fig. 7A), suggesting similar availability of labeled acetate substrate for their synthesis. These results, therefore, suggest that cumulus cells provide oocytes with newly synthesized cholesterol. Support for this conclusion is the observation that lower levels of [^{14}C]cholesterol were detected in DM cumulus-cell-enclosed oocytes compared with WT oocytes, and levels of [^{14}C]cholesterol in DM oocytes were partially promoted by co-culture of DM cumulus-cell-enclosed oocytes with WT oocytes (Fig. 7B). These changes in DM oocytes are coincident with changes in [^{14}C]cholesterol levels in DM cumulus cells (Fig. 7C). Cumulus cells were collected from the same COCs used for measuring levels of [^{14}C]cholesterol in oocytes (Fig. 7B).

DISCUSSION

The transcriptome of cumulus cells before the LH surge was highly affected by deletion of *Bmp15*, and this effect was enhanced in *Bmp15*$^{-/-}$ *Gdf9*$^{+/-}$ (DM) mice. Thus both BMP15 and GDF9 are important regulators of cumulus cell development and function before the LH surge. The most highly affected processes were metabolic, with glycolysis and sterol biosynthesis affected most dramatically. These effects could reflect acute regulation of these transcripts by oocytes, rather than an effect of chronic deprivation of BMP15 and GDF9 throughout follicular development, because removal of the oocyte from WT COCs results in the same alterations in steady-state transcript levels as observed in mutant cumulus cells. Synthesis of cholesterol from acetate was reduced by removal of oocytes from WT COCs and in cumulus cells of mutant mice. Two

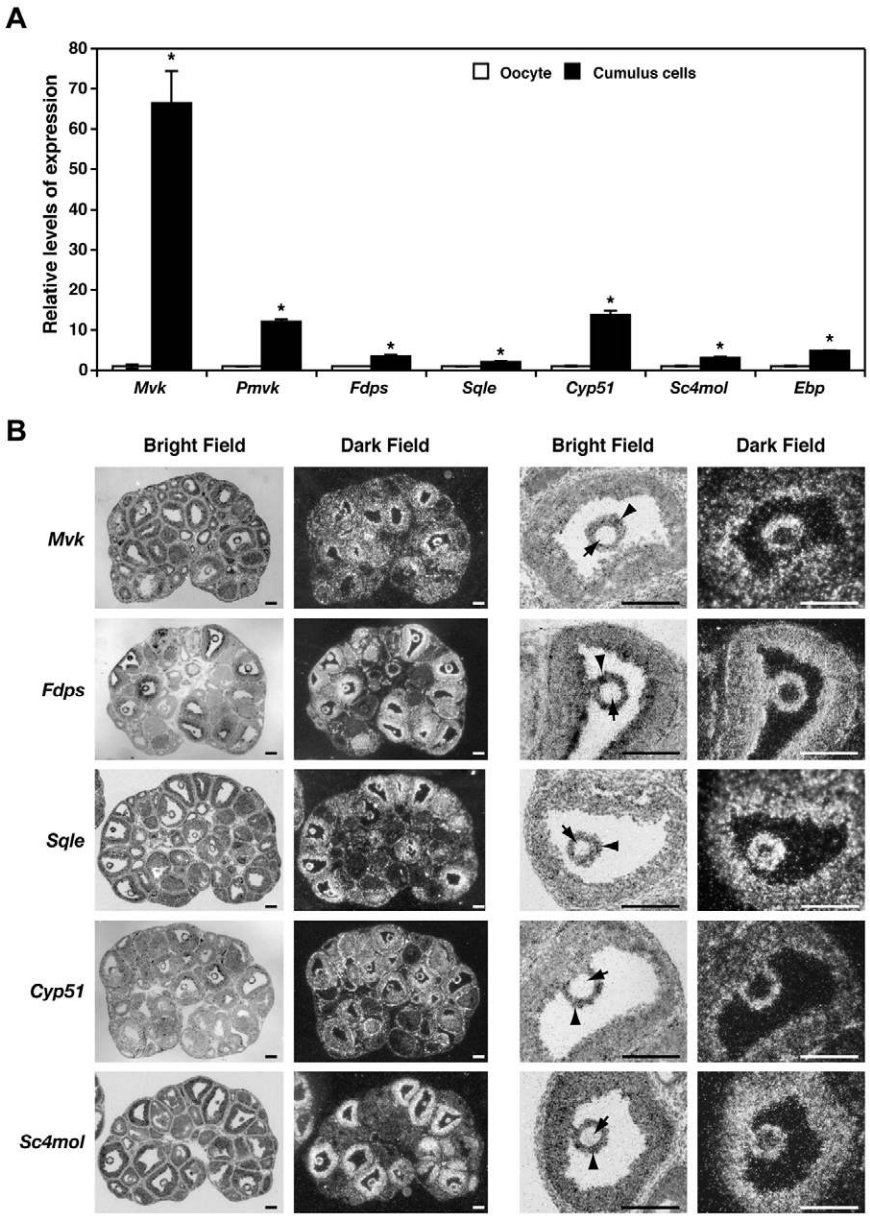

Fig. 6. Comparison of expression of transcripts encoding enzymes required for cholesterol biosynthesis in oocytes and cumulus cells. (**A**) Comparison of mRNA levels of transcripts encoding enzymes required for cholesterol biosynthesis in oocytes and cumulus cells, relative to levels of *Rpl19* mRNA expressed by those cell types. Experiment was repeated three times independently. Data are presented as mean of the fold change of the mRNA levels relative to levels in oocytes (given a value of 1) ± s.e.m. **P*<0.05, compared with levels in oocytes. (**B**) In situ hybridization of transcripts encoding enzymes required for cholesterol biosynthesis. The four images in each row show localization of transcripts indicated on the left side. In each row, the first two panels (from left) are low magnification, bright- and dark-field images of a 22-day-old eCG-primed ovary; the last two panels are high magnification, bright- and dark-field images of large antral follicles from the same ovary. Cumulus cells and oocyte in each follicle are indicated by an arrowhead and an arrow, respectively. Scale bars: 200 μm.

lines of evidence indicate that mouse oocytes are deficient in their ability to synthesize cholesterol. First, levels of expression of transcripts encoding enzymes of the cholesterol synthesis pathway were very low in oocytes compared with cumulus cells. Second, cumulus-cell-denuded oocytes convert acetate to cholesterol poorly. Thus oocytes probably depend upon cumulus cells to provide them with cholesterol, and oocytes stimulate this activity in cumulus cells via BMP15 and GDF9. Supporting this conclusion, lower levels of radiolabeled cholesterol were detected in cumulus-cell-enclosed DM oocytes, which was coincident with the reduced ability of DM cumulus cells to synthesize cholesterol. Co-culture of the DM complexes with fully grown WT oocytes partially restored levels of radiolabeled cholesterol in both DM cumulus cells and oocytes.

The glycolysis/gluconeogenesis pathway is highly affected in cumulus cells by *Bmp15* and *Gdf9* mutation. Steady-state levels of most of transcripts encoding enzymes of the glycolytic pathway were decreased in both *Bmp15*$^{-/-}$ and DM cumulus cells. That oocytes control glycolysis in cumulus cells was known from previous studies (Sugiura et al., 2005), but the breadth of impact of oocytes on expression of diverse transcripts encoding enzymes needed for this pathway had not been realized prior to this analysis of mutant cumulus cell transcriptomes.

As indicated above, effects of *Bmp15*$^{-/-}$ and DM on expression of transcripts encoding enzymes required for glycolysis in cumulus cells was anticipated based on previous studies (Sugiura et al., 2005). By contrast, the effects of these mutations on cholesterol biosynthesis in cumulus cells was entirely unexpected. Almost all (13/17) transcripts encoding enzymes required for cholesterol biosynthesis were downregulated in cumulus cells of both mutants, and this correlated with a reduction of de-novo-synthesized cholesterol from acetate. Therefore, BMP15 and GDF9 control the rate of cholesterol biosynthesis in cumulus cells at least in part by promoting expression of transcripts encoding cholesterol biosynthetic enzymes. Removal of oocytes resulted in downregulation in levels of 15/17 of transcripts in this pathway, as well as reduction in cholesterol synthesis in cumulus cells without oocytes. Co-culture of OOX cumulus cells with WT oocytes completely prevented the decrease in steady-state transcript levels in WT OOX cumulus cells. Although cholesterol

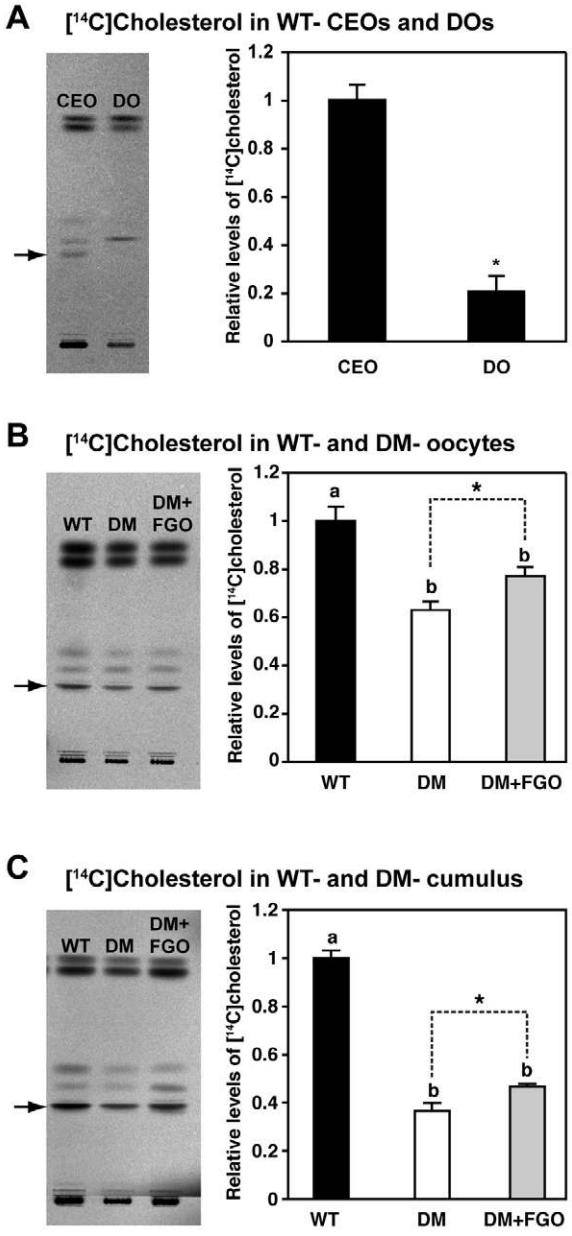

Fig. 7. Comparison of levels of cholesterol synthesized in oocytes and/or cumulus cells under various experimental conditions. (**A**) Comparison of levels of cholesterol synthesized in WT cumulus-cell-enclosed oocytes (CEOs) and denuded oocytes (DOs). The left panel is a representative TLC image showing levels of [^{14}C]cholesterol (indicated by arrow) production in CEO and DOs. The right panel is the quantitative comparison of [^{14}C]cholesterol levels in CEOs and DOs. (**B**) Comparison of levels of cholesterol synthesized in oocytes of WT, DM cumulus-oocyte complexes (COCs), and DM COCs that were co-cultured with WT fully grown oocytes (FGOs). The left panel is a representative TLC image showing levels of [^{14}C]cholesterol (indicated by arrow) produced by oocytes in each group. The right panel is the quantitative comparison of [^{14}C]cholesterol levels in oocytes of each group. (**C**) Comparison of levels of cholesterol synthesized in cumulus cells of WT, DM COCs, and DM COCs that were co-cultured with WT FGOs. The left panel is a representative TLC image showing levels of [^{14}C]cholesterol (indicated by arrow) produced by cumulus in each group. The right panel is the quantitative comparison of [^{14}C]cholesterol levels produced by cumulus cells in each group. All experiments were repeated four times. Data are presented as mean of the relative fold change in [^{14}C]cholesterol levels (levels in controls, i.e., CEO in A, WT in B and C,=1) ± s.e.m. Bars indicated with different letters are significantly different (P<0.05) using ANOVA and Tukey's HSD test. The asterisk indicates significant difference by Student's t-test (P<0.05).

synthesis still decreased in OOX cumulus cells co-cultured with oocytes, synthesis did not decrease to levels found in OOX cumulus cells not co-cultured with oocytes. Thus oocytes acutely promote cholesterol biosynthesis in cumulus cells. Although oocyte-derived factors, probably including BMP15 and GDF9, promote the expression of transcripts encoding enzymes essential for cholesterol synthesis, it appears that an additional interaction between oocytes and cumulus cells is necessary for full capacity to synthesize cholesterol. This additional interaction appears to require contact between oocytes and cumulus cells.

Cholesterol 27 hydroxylase, CYP27A1, functions mainly in liver, converting cholesterol to bile acids (Bjorkhem, 1992). The steady-state level of *Cyp27a1* mRNA was markedly elevated in *Bmp15*$^{-/-}$ and DM cumulus cells and also in WT cumulus cells without oocytes. Oocytes, via BMP15 and GDF9, could therefore suppress cholesterol degradation in cumulus cells and provide another avenue, besides promoting cholesterol biosynthesis, for promoting elevation of cholesterol levels in cumulus cells.

In general, cells accumulate cholesterol from two sources: de-novo synthesis and uptake of extracellular cholesterol via specific receptors for cholesterol carriers. Since evidence is presented here that oocytes are deficient in their ability to produce cholesterol using an endogenous synthetic pathway, they could, theoretically, acquire cholesterol via uptake from their micro-environment via receptor-mediated selective uptake. However, receptors for either HDL-cholesterol (i.e. SCARB1, scavenger receptor class B, member 1, also known as SR-BI) or LDL-cholesterol (i.e. LDLR) are not expressed by mouse oocytes (Sato et al., 2003; Trigatti et al., 1999) suggesting that mouse oocytes are unable to take up carrier-borne cholesterol. What is the source of oocyte cholesterol needed for oocyte development and subsequent embryogenesis? Although cholesterol synthesis was very low in denuded oocytes, much more radiolabeled cholesterol was found in cumulus-cell-enclosed oocytes suggesting that cholesterol was first synthesized by cumulus cells and then transferred to oocytes. It could be argued that cumulus cells stimulate oocytes to synthesize cholesterol. However, this is unlikely because of the poor expression of transcripts encoding the enzymes required for cholesterol synthesis in oocytes. We therefore conclude that a portion of the cholesterol that is either produced or taken up by cumulus cells is transferred to oocytes and that cumulus cells are the source of cholesterol for mouse oocytes.

Do cumulus cells themselves synthesize all of the cholesterol destined for oocytes? SCARB1 is a receptor of HDL cholesterol (Acton et al., 1996). Expression of *Scarb1* mRNA was reported to be restricted to theca cells before the LH surge, and detected in granulosa cells only after the LH surge (Li et al., 1998). However, our analysis of the WT cumulus cell transcriptome shows expression of both *Scarb1* and *Ldlr* mRNA. It is therefore possible that these receptors could take up oocyte-destined cholesterol into cumulus cells. However, little LDL cholesterol is present in follicular fluid (Perret et al., 1985; Simpson et al., 1980). Moreover, deletion of *Ldlr* does not affect fertility in mice (Ishibashi et al., 1993). *Scarb1*$^{-/-}$ female mice are infertile (Trigatti et al., 1999). However, the

infertility can be reversed by transplanting *Scarb1*$^{-/-}$ ovaries to ovariectomized WT recipients, or by lowering the elevated level of plasma cholesterol in *Scarb1*$^{-/-}$ mice with the HDL cholesterol-lowering drug probutol (Miettinen et al., 2001). Thus infertility of *Scarb1*$^{-/-}$ females is not caused by the absence of SCARB1 in the ovary, but rather indirectly by extra-ovarian defects resulting from the absence of SCARB1 (Miettinen et al., 2001). Therefore, although some cholesterol destined for transfer to oocytes could be taken up initially by cumulus cells, cholesterol synthesized by the cumulus cells may be the main source of oocyte cholesterol.

Cholesterol-enriched lipid rafts are present in membranes of mouse oocytes and preimplantation embryos, and treating zygotes with the cholesterol-depleting drug, methyl-β-cyclodextrin, prevented embryonic development beyond 2- to 4-cell stages in culture (Comiskey and Warner, 2007). This indicates that cholesterol deposition in mouse oocytes and embryos is essential for supporting preimplantation development. Furthermore, earlier studies suggested that the full sterol synthetic pathway, i.e., the ability to convert acetate to cholesterol, is not operative in mouse preimplantation embryos until the blastocyst stage (Pratt, 1978; Pratt, 1982). Therefore, cholesterol and other sterols stored in oocytes are probably required for preimplantation development. Results presented here indicate that cumulus cells provide this cholesterol to oocytes. Therefore, mouse oocytes are promoting their own developmental competence by stimulating cholesterol synthesis in cumulus cells, some of which is then provided to oocytes. Preimplantation development was significantly delayed in DM mice (Su et al., 2004), and this delay could result, at least in part, from lower levels of cholesterol provided to DM oocytes.

We thank Sonya Kamdar and the Jackson Laboratory Gene Expression Service for help with microarray studies, Robert Wilpan of the Protein Chemistry Service for providing facilities and equipment needed for TLC; Anders Friberg and Håkan Billig, Göteborg University, Sweden, for kindly sharing protocols for analysis of cholesterol synthesis in granulosa cells, Bernard Fried, Lafayette College for helpful advice on TLC techniques, and Tom Gridley and Mary Ann Handel for comments and suggestions on this manuscript. Funding was supplied by the following grants: HD23839 (Y.-Q.S., K.S., J.J.E.), HD21970 (K.S., K.W., M.J.O., J.J.E.), HD33438 (S.A.P., M.M.M.) and 5F32HD46335 (S.A.P.). The Jackson Laboratory Gene Expression Facility is supported by HL072241/Shared Microarray Facilities grant.

Supplementary material

Supplementary material for this article is available at
http://dev.biologists.org/cgi/content/full/135/1/111/DC1

References

Acton, S., Rigotti, A., Landschulz, K. T., Xu, S., Hobbs, H. H. and Krieger, M. (1996). Identification of scavenger receptor SR-BI as a high density lipoprotein receptor. *Science* **271**, 518-520.

Biggers, J. D., Whittingham, D. G. and Donahue, R. P. (1967). The pattern of energy metabolism in the mouse oocyte and zygote. *Proc. Natl. Acad. Sci. USA* **58**, 560-567.

Bjorkhem, I. (1992). Mechanism of degradation of the steroid side chain in the formation of bile acids. *J. Lipid Res.* **33**, 455-471.

Bodin, L., Di Pasquale, E., Fabre, S., Bontoux, M., Monget, P., Persani, L. and Mulsant, P. (2007). A novel mutation in the bone morphogenetic protein 15 gene causing defective protein secretion is associated with both increased ovulation rate and sterility in Lacaune sheep. *Endocrinology* **148**, 393-400.

Buccione, R., Vanderhyden, B. C., Caron, P. J. and Eppig, J. J. (1990). FSH-induced expansion of the mouse cumulus oophorus in vitro is dependent upon a specific factor(s) secreted by the oocyte. *Dev. Biol.* **138**, 16-25.

Chand, A. L., Ponnampalam, A. P., Harris, S. E., Winship, I. M. and Shelling, A. N. (2006). Mutational analysis of BMP15 and GDF9 as candidate genes for premature ovarian failure. *Fertil. Steril.* **86**, 1009-1012.

Colonna, R. and Mangia, F. (1983). Mechanisms of amino acid uptake in cumulus-enclosed mouse oocytes. *Biol. Reprod.* **28**, 797-803.

Comiskey, M. and Warner, C. M. (2007). Spatio-temporal localization of membrane lipid rafts in mouse oocytes and cleaving preimplantation embryos. *Dev. Biol.* **303**, 727-739.

Cui, X. and Churchill, G. A. (2003). Statistical tests for differential expression in cDNA microarray experiments. *Genome Biol.* **4**, 210.

Cui, X., Hwang, J. T., Qiu, J., Blades, N. J. and Churchill, G. A. (2005). Improved statistical tests for differential gene expression by shrinking variance components estimates. *Biostatistics* **6**, 59-75.

Di Pasquale, E., Rossetti, R., Marozzi, A., Bodega, B., Borgato, S., Cavallo, L., Einaudi, S., Radetti, G., Russo, G., Sacco, M. et al. (2006). Identification of new variants of human BMP15 gene in a large cohort of women with premature ovarian failure. *J. Clin. Endocrinol. Metab.* **91**, 1976-1979.

Diaz, F. J., O'Brien, M. J., Wigglesworth, K. and Eppig, J. J. (2006). The preantral granulosa cell to cumulus cell transition in the mouse ovary: development of competence to undergo expansion. *Dev. Biol.* **299**, 91-104.

Diaz, F. J., Wigglesworth, K. and Eppig, J. J. (2007a). Oocytes are required for the preantral granulosa cell to cumulus cell transition in mice. *Dev. Biol.* **305**, 300-311.

Diaz, F. J., Wigglesworth, K. and Eppig, J. J. (2007b). Oocytes determine cumulus cell lineage in mouse ovarian follicles. *J. Cell Sci.* **120**, 1330-1340.

Dixit, H., Rao, L. K., Padmalatha, V. V., Kanakavalli, M., Deenadayal, M., Gupta, N., Chakrabarty, B. and Singh, L. (2006). Missense mutations in the BMP15 gene are associated with ovarian failure. *Hum. Genet.* **119**, 408-415.

Donahue, R. P. and Stern, S. (1968). Follicular cell support of oocyte maturation: production of pyruvate in vitro. *J. Reprod. Fertil.* **17**, 395-398.

Dong, J., Albertini, D. F., Nishimori, K., Kumar, T. R., Lu, N. and Matzuk, M. M. (1996). Growth differentiation factor-9 is required during early ovarian folliculogenesis. *Nature* **383**, 531-535.

Dragovic, R. A., Ritter, L. J., Schulz, S. J., Amato, F., Armstrong, D. T. and Gilchrist, R. B. (2005). Role of oocyte-secreted growth differentiation factor 9 in the regulation of mouse cumulus expansion. *Endocrinology* **146**, 2798-2806.

Dragovic, R. A., Ritter, L. J., Schulz, S. J., Amato, F., Thompson, J. G., Armstrong, D. T. and Gilchrist, R. B. (2007). Oocyte-secreted factor activation of SMAD 2/3 signaling enables initiation of mouse cumulus cell expansion. *Biol. Reprod.* **76**, 848-857.

Elvin, J. A., Clark, A. T., Wang, P., Wolfman, N. M. and Matzuk, M. M. (1999a). Paracrine actions of growth differentiation factor-9 in the mammalian ovary. *Mol. Endocrinol.* **13**, 1035-1048.

Elvin, J. A., Yan, C. N., Wang, P., Nishimori, K. and Matzuk, M. M. (1999b). Molecular characterization of the follicle defects in the growth differentiation factor 9-deficient ovary. *Mol. Endocrinol.* **13**, 1018-1034.

Elvin, J. A., Yan, C. N. and Matzuk, M. M. (2000). Growth differentiation factor-9 stimulates progesterone synthesis in granulosa cells via a prostaglandin E-2/EP2 receptor pathway. *Proc. Natl. Acad. Sci. USA* **97**, 10288-10293.

Eppig, J. J. (2001). Oocyte control of ovarian follicular development and function in mammals. *Reproduction* **122**, 829-838.

Eppig, J. J., Wigglesworth, K. and Pendola, F. L. (2002). The mammalian oocyte orchestrates the rate of ovarian follicular development. *Proc. Natl. Acad. Sci. USA* **99**, 2890-2894.

Eppig, J. J., Pendola, F. L., Wigglesworth, K. and Pendola, J. K. (2005). Mouse oocytes regulate metabolic cooperativity between granulosa cells and oocytes: amino acid transport. *Biol. Reprod.* **73**, 351-357.

Erickson, G. F. and Shimasaki, S. (2001). The physiology of folliculogenesis: the role of novel growth factors. *Fertil. Steril.* **76**, 943-949.

Friberg, P. A., Larsson, D. G., Rung, E. and Billig, H. (2007). Apoptotic effects of a progesterone receptor antagonist on rat granulosa cells are not mediated via reduced protein isoprenylation. *Mol. Reprod. Dev.* **74**, 1317-1326.

Galloway, S. M., McNatty, K. P., Cambridge, L. M., Laitinen, M. P. E., Juengel, J. L., Jokiranta, T. S., McLaren, R. J., Luiro, K., Dodds, K. G., Montgomery, G. W. et al. (2000). Mutations in an oocyte-derived growth factor gene (BMP15) cause increased ovulation rate and infertility in a dosage-sensitive manner. *Nat. Genet.* **25**, 279-283.

Gautier, L., Cope, L. M., Bolstad, B. M. and Irizarry, R. A. (2004). Affy – analysis of Affymetrix GeneChip data at the probe level. *Bioinformatics* **20**, 307-315.

Gilchrist, R. B., Ritter, L. J. and Armstrong, D. G. (2000). Growth-promoting activity of mouse oocytes is developmentally regulated. *Biol. Reprod.* **62**, 272.

Gilchrist, R. B., Ritter, L. J. and Armstrong, D. G. (2001). Mouse oocyte mitogenic activity is developmentally coordinated throughout folliculogenesis and meiotic maturation. *Dev. Biol.* **240**, 289-298.

Gilchrist, R. B., Morrissey, M. P., Ritter, L. J. and Armstrong, D. T. (2003). Comparison of oocyte factors and transforming growth factor-beta in the regulation of DNA synthesis in bovine granulosa cells. *Mol. Cell. Endocrinol.* **201**, 87-95.

Gu, S., Roderick, H. L., Camacho, P. and Jiang, J. X. (2000). Identification and characterization of an amino acid transporter expressed differentially in liver. *Proc. Natl. Acad. Sci. USA* **97**, 3230-3235.

Gueripel, X., Brun, V. and Gougeon, A. (2006). Oocyte bone morphogenetic protein 15, but not growth differentiation factor 9, is increased during gonadotropin-induced follicular development in the immature mouse and is associated with cumulus oophorus expansion. *Biol. Reprod.* **75**, 836-843.

Haghighat, N. and Van Winkle, L. J. (1990). Developmental change in follicular cell-enhanced amino acid uptake into mouse oocytes that depends on intact gap junctions and transport system Gly. *J. Exp. Zool.* **253**, 71-82.

Hayashi, M., McGee, E. A., Min, G., Klein, C., Rose, U. M., van Duin, M. and Hsueh, A. J. (1999). Recombinant growth differentiation factor-9 (GDF-9) enhances growth and differentiation of cultured early ovarian follicles. *Endocrinology* **140**, 1236-1244.
Hussein, T. S., Froiland, D. A., Amato, F., Thompson, J. G. and Gilchrist, R. B. (2005). Oocytes prevent cumulus cell apoptosis by maintaining a morphogenic paracrine gradient of bone morphogenetic proteins. *J. Cell Sci.* **118**, 5257-5268.
Irizarry, R. A., Bolstad, B. M., Collin, F., Cope, L. M., Hobbs, B. and Speed, T. P. (2003). Summaries of Affymetrix GeneChip probe level data. *Nucleic Acids Res.* **31**, e15.
Ishibashi, S., Brown, M. S., Goldstein, J. L., Gerard, R. D., Hammer, R. E. and Herz, J. (1993). Hypercholesterolemia in low density lipoprotein receptor knockout mice and its reversal by adenovirus-mediated gene delivery. *J. Clin. Invest.* **92**, 883-893.
Joyce, I. M., Pendola, F. L., O'Brien, M. and Eppig, J. J. (2001). Regulation of prostaglandin-endoperoxide synthase 2 messenger ribonucleic acid expression in mouse granulosa cells during ovulation. *Endocrinology* **142**, 3187-3197.
Juengel, J. L. and McNatty, K. P. (2005). The role of proteins of the transforming growth factor-beta superfamily in the intraovarian regulation of follicular development. *Hum. Reprod. Update* **11**, 143-160.
Juengel, J. L., Hudson, N. L., Heath, D. A., Smith, P., Reader, K. L., Lawrence, S. B., O'Connell, A. R., Laitinen, M. P. E., Cranfield, M., Groome, N. P. et al. (2002). Growth differentiation factor 9 and bone morphogenetic protein 15 are essential for ovarian follicular development in sheep. *Biol. Reprod.* **67**, 1777-1789.
Latham, K. E., Wigglesworth, K., McMenamin, M. and Eppig, J. J. (2004). Stage-dependent effects of oocytes and growth differentiation factor 9 on mouse granulosa cell development: advance programming and subsequent control of the transition from preantral secondary follicles to early antral tertiary follicles. *Biol. Reprod.* **70**, 1253-1262.
Leese, H. J. and Barton, A. M. (1984). Pyruvate and glucose uptake by mouse ova and preimplantation embryos. *J. Reprod. Fertil.* **72**, 9-13.
Leese, H. J. and Barton, A. M. (1985). Production of pyruvate by isolated mouse cumulus cells. *J. Exp. Zool.* **234**, 231-236.
Li, H. K., Kuo, T. Y., Yang, H. S., Chen, L. R., Li, S. S. and Huang, H. W. (2006). Differential gene expression of bone morphogenetic protein 15 and growth differentiation factor 9 during in vitro maturation of porcine oocytes and early embryos. *Anim. Reprod. Sci.* doi:10.1016/j.anireprosci.2006.12.017.
Li, X., Peegel, H. and Menon, K. M. (1998). In situ hybridization of high density lipoprotein (scavenger, type 1) receptor messenger ribonucleic acid (mRNA) during folliculogenesis and luteinization: evidence for mRNA expression and induction by human chorionic gonadotropin specifically in cell types that use cholesterol for steroidogenesis. *Endocrinology* **139**, 3043-3049.
Matzuk, M. M., Burns, K. H., Viveiros, M. M. and Eppig, J. J. (2002). Intercellular communication in the mammalian ovary: oocytes carry the conversation. *Science* **296**, 2178-2180.
McNatty, K. P., Moore, L. G., Hudson, N. L., Quirke, L. D., Lawrence, S. B., Reader, K., Hanrahan, J. P., Smith, P., Groome, N. P., Laitinen, M. et al. (2004). The oocyte and its role in regulating ovulation rate: a new paradigm in reproductive biology. *Reproduction* **128**, 379-386.
McNatty, K. P., Juengel, J. L., Reader, K. L., Lun, S., Myllymaa, S., Lawrence, S. B., Western, A., Meerasahib, M. F., Mottershead, D. G., Groome, N. P. et al. (2005a). Bone morphogenetic protein 15 and growth differentiation factor 9 co-operate to regulate granulosa cell function. *Reproduction* **129**, 473-480.
McNatty, K. P., Juengel, J. L., Reader, K. L., Lun, S., Myllymaa, S., Lawrence, S. B., Western, A., Meerasahib, M. F., Mottershead, D. G., Groome, N. P. et al. (2005b). Bone morphogenetic protein 15 and growth differentiation factor 9 co-operate to regulate granulosa cell function in ruminants. *Reproduction* **129**, 481-487.
Miettinen, H. E., Rayburn, H. and Krieger, M. (2001). Abnormal lipoprotein metabolism and reversible female infertility in HDL receptor (SR-BI)-deficient mice. *J. Clin. Invest.* **108**, 1717-1722.
Orisaka, M., Orisaka, S., Jiang, J. Y., Craig, J., Wang, Y., Kotsuji, F. and Tsang, B. K. (2006). Growth differentiation factor 9 is antiapoptotic during follicular development from preantral to early antral stage. *Mol. Endocrinol.* **20**, 2456-2468.
Otsuka, F. and Shimasaki, S. (2002). A negative feedback system between oocyte bone morphogenetic protein 15 and granulosa cell kit ligand: its role in regulating granulosa cell mitosis. *Proc. Natl. Acad. Sci. USA* **99**, 8060-8065.
Otsuka, F., Yao, Z., Lee, T., Yamamoto, S., Erickson, G. F. and Shimasaki, S. (2000). Bone morphogenetic protein-15. Identification of target cells and biological functions. *J. Biol. Chem.* **275**, 39523-39528.
Otsuka, F., Moore, R. K. and Shimasaki, S. (2001a). Biological function and cellular mechanism of bone morphogenetic protein-6 in the ovary. *J. Biol. Chem.* **276**, 32889-32895.
Otsuka, F., Yamamoto, S., Erickson, G. F. and Shimasaki, S. (2001b). Bone morphogenetic protein-15 inhibits follicle-stimulating hormone (FSH) action by suppressing FSH receptor expression. *J. Biol. Chem.* **276**, 11387-11392.
Otsuka, F., Moore, R. K., Wang, X., Sharma, S., Miyoshi, T. and Shimasaki, S. (2005). Essential role of the oocyte in estrogen amplification of follicle-stimulating hormone signaling in granulosa cells. *Endocrinology* **146**, 3362-3367.
Palmer, J. S., Zhao, Z. Z., Hoekstra, C., Hayward, N. K., Webb, P. M., Whiteman, D. C., Martin, N. G., Boomsma, D. I., Duffy, D. L. and Montgomery, G. W. (2006). Novel variants in growth differentiation factor 9 in mothers of dizygotic twins. *J. Clin. Endocrinol. Metab.* **91**, 4713-4716.
Pangas, S. A. and Matzuk, M. M. (2004). Genetic models for transforming growth factor beta superfamily signaling in ovarian follicle development. *Mol. Cell. Endocrinol.* **225**, 83-91.
Pangas, S. A. and Matzuk, M. M. (2005). The art and artifact of GDF9 activity: cumulus expansion and the cumulus expansion-enabling factor. *Biol. Reprod.* **73**, 582-585.
Perret, B. P., Parinaud, J., Ribbes, H., Moatti, J. P., Pontonnier, G., Chap, H. and Douste-Blazy, L. (1985). Lipoprotein and phospholipid distribution in human follicular fluids. *Fertil. Steril.* **43**, 405-409.
Pratt, H. P. (1978). Lipids and transitions in embryos. In *Development in Mammals*. Vol. 3 (ed. M. H. Johnson), pp. 83-129. Amsterdam, New York, Oxford: Elsevier, North-Holland.
Pratt, H. P. (1982). Preimplantation mouse embryos synthesize membrane sterols. *Dev. Biol.* **89**, 101-110.
Rung, E., Friberg, P. A., Shao, R., Larsson, D. G., Nielsen, E., Svensson, P. A., Carlsson, B., Carlsson, L. M. and Billig, H. (2005). Progesterone-receptor antagonists and statins decrease de novo cholesterol synthesis and increase apoptosis in rat and human periovulatory granulosa cells in vitro. *Biol. Reprod.* **72**, 538-545.
Rung, E., Friberg, P. A., Bergh, C. and Billig, H. (2006). Depletion of substrates for protein prenylation increases apoptosis in human periovulatory granulosa cells. *Mol. Reprod. Dev.* **73**, 1277-1283.
Sato, N., Kawamura, K., Fukuda, J., Honda, Y., Sato, T., Tanikawa, H., Kodama, H. and Tanaka, T. (2003). Expression of LDL receptor and uptake of LDL in mouse preimplantation embryos. *Mol. Cell. Endocrinol.* **202**, 191-194.
Simpson, E. R., Rochelle, D. B., Carr, B. R. and MacDonald, P. C. (1980). Plasma lipoproteins in follicular fluid of human ovaries. *J. Clin. Endocrinol. Metab.* **51**, 1469-1471.
Soyal, S. M., Amleh, A. and Dean, J. (2000). FIGa, a germ cell-specific transcription factor required for ovarian follicle formation. *Development* **127**, 4645-4654.
Storey, J. D. and Tibshirani, R. (2003). Statistical significance for genomewide studies. *Proc. Natl. Acad. Sci. USA* **100**, 9440-9445.
Su, Y. Q., Wu, X., O'Brien, M. J., Pendola, F. L., Denegre, J. N., Matzuk, M. M. and Eppig, J. J. (2004). Synergistic roles of BMP15 and GDF9 in the development and function of the oocyte-cumulus cell complex in mice: genetic evidence for an oocyte-granulosa cell regulatory loop. *Dev. Biol.* **276**, 64-73.
Su, Y. Q., Sugiura, K., Woo, Y., Wigglesworth, K., Kamdar, S., Affourtit, J. and Eppig, J. J. (2007). Selective degradation of transcripts during meiotic maturation of mouse oocytes. *Dev. Biol.* **302**, 104-117.
Sugiura, K. and Eppig, J. J. (2005). Control of metabolic cooperativity between oocytes and their companion granulosa cells by mouse oocytes. *Reprod. Fertil. Dev.* **17**, 667-674.
Sugiura, K., Pendola, F. L. and Eppig, J. J. (2005). Oocyte control of metabolic cooperativity between oocytes and companion granulosa cells: energy metabolism. *Dev. Biol.* **279**, 20-30.
Trigatti, B., Rayburn, H., Vinals, M., Braun, A., Miettinen, H., Penman, M., Hertz, M., Schrenzel, M., Amigo, L., Rigotti, A. et al. (1999). Influence of the high density lipoprotein receptor SR-BI on reproductive and cardiovascular pathophysiology. *Proc. Natl. Acad. Sci. USA* **96**, 9322-9327.
Vanderhyden, B. C., Caron, P. J., Buccione, R. and Eppig, J. J. (1990). Developmental pattern of the secretion of cumulus-expansion enabling factor by mouse oocytes and the role of oocytes in promoting granulosa cell differentiation. *Dev. Biol.* **140**, 307-317.
Vanderhyden, B. C., Telfer, E. E. and Eppig, J. J. (1992). Mouse oocytes promote proliferation of granulosa cells from preantral and antral follicles in vitro. *Biol. Reprod.* **46**, 1196-1204.
Vitt, U. A., Hayashi, M., Klein, C. and Hsueh, A. J. (2000). Growth differentiation factor-9 stimulates proliferation but suppresses the follicle-stimulating hormone-induced differentiation of cultured granulosa cells from small antral and preovulatory rat follicles. *Biol. Reprod.* **62**, 370-377.
Wu, H., Kerr, M. K., Cui, X. and Churchill, G. A. (2003). MAANOVA: a software package for the analysis of spotted cDNA microarray experiments. In *The Analysis of Gene Expression Data: An Overview of Methods and Software* (ed. G. Parmigiani, E. S. Garett, R. A. Irizarry and S. L. Zeger), pp. 313-431. New York: Springer.
Yan, C., Wang, P., DeMayo, J., DeMayo, F. J., Elvin, J. A., Carino, C., Prasad, S. V., Skinner, S. S., Dunbar, B. S., Dube, J. L. et al. (2001). Synergistic roles of bone morphogenetic protein 15 and growth differentiation factor 9 in ovarian function. *Mol. Endocrinol.* **15**, 854-866.
Yoshino, O., McMahon, H. E., Sharma, S. and Shimasaki, S. (2006). A unique preovulatory expression pattern plays a key role in the physiological functions of BMP-15 in the mouse. *Proc. Natl. Acad. Sci. USA* **103**, 10678-10683.